

$t\bar{t}b\bar{b}$ hadroproduction with massive bottom quarks with PowHelG. Bevilacqua,¹ M.V. Garzelli,² and A. Kardos³¹*MTA-DE Particle Physics Research Group, University of Debrecen, H-4010 Debrecen, PBox 105, Hungary*²*Institute for Theoretical Physics, University of Hamburg,**Luruper Chaussee 149, D-22761 Hamburg, Germany*³*Department of Experimental Physics, University of Debrecen, H-4010 Debrecen, PBox 105, Hungary*

(Dated: September 4, 2018)

The associated production of top-antitop-bottom-antibottom quarks is a relevant irreducible background for Higgs boson analyses in the top-antitop-Higgs production channel, with Higgs decaying into a bottom-antibottom quark pair. We implement this process in the `PowHel` event generator, considering the bottom quarks as massive in all steps of the computation which involves hard-scattering matrix-elements in the 4-flavour number scheme combined with 4-flavour Parton Distribution Functions. Predictions with NLO QCD + Parton Shower accuracy, as obtained by `PowHel` + `PYTHIA`, are compared to those which resulted from a previous `PowHel` implementation with hard-scattering matrix-elements in the 5-flavour number scheme, considering as a baseline the example of a realistic analysis of top-antitop hadroproduction with additional b -jet activity, performed by the CMS collaboration at the Large Hadron Collider.

PACS numbers: 12.38.-t - Quantum ChromoDynamics, 14.65.Ha - Top quarks, 14.65.Fy - Bottom quarks

I. INTRODUCTION

Top-antitop-bottom-antibottom ($t\bar{t}b\bar{b}$) hadroproduction is a process of interest for collider phenomenology, first of all because it is an irreducible background to $t\bar{t}H$ hadroproduction with the Higgs boson decaying into a $b\bar{b}$ pair [1–3]. However, the experimental determination of its cross-section is characterized by a series of challenges, related on the one hand to its smallness, and on the other hand to the fact that the separation of the $t\bar{t}b\bar{b}$ signal from its dominant backgrounds of a $t\bar{t}$ -quark pair accompanied by a couple of charm- or light-jets relies on b -tagging, involving many uncertainties. A reliable theoretical modelling of this process is thus necessary even in experimental studies. Indeed, even this modelling represents a challenge, because $t\bar{t}b\bar{b}$ is a multileg and multiscale process. This has boosted theoretical developments and advances in computational techniques.

Theory predictions for $t\bar{t}b\bar{b}$ hadroproduction including next-to-leading-order (NLO) QCD radiative corrections were first presented in 2009, by two independent groups [4–6], relying on different techniques to compute 1-loop amplitudes (tensor integral reduction vs. OPP reduction). In both calculations the 5-flavour number scheme (5 FNS) was adopted, with b -quarks assumed to be massless, and the bottom appearing as an active flavour in the parton distribution functions (PDF). The computation of Ref. [5], performed with the `Helac-NLO` event generator (`Helac-1loop` + `Helac-Dipoles`, see Ref. [7] and references therein, in particular the earlier developments described in Ref. [8–10]), was subsequently matched to Parton Shower (PS) [11], using the POWHEG matching formalism [12, 13], as implemented in the POWHEG-BOX framework [14]. In particular, the `PowHel` $t\bar{t}b\bar{b}$ generator was developed [11, 15], which relies on amplitudes computed by the `Helac-1loop` framework, used as input for POWHEG-BOX. In `PowHel` the

subtraction of infrared divergences has been performed through the FKS formalism [16], as implemented in POWHEG-BOX, differently from `Helac-NLO`, which, in its first formulation, adopted the Catani-Seymour dipole formalism [10, 17, 18]. Events generated by `PowHel`, delivered in the Les Houches Event Format (LHE) [19], and subsequently showered by different Shower Monte Carlo generators (SMC), were used by both the ATLAS and CMS experimental collaborations to analyze data collected at the Large Hadron Collider (LHC) at $\sqrt{s} = 8$ TeV [20, 21]. In those `PowHel` LHE events, involving up to an additional radiation emission, b -quarks were assumed to be massless, whereas their mass was included and accounted for in the remaining SMC evolution.

After the appearance of Ref. [11], differential cross-sections for $t\bar{t}b\bar{b}$ hadroproduction at both NLO QCD and at NLO QCD + PS accuracy, retaining the mass of the bottom quarks already in the hard-scattering matrix-elements (4 FNS), were presented for the first time in a dedicated paper [22] on the basis of `OpenLoops` + `SHERPA`, considering the case of stable top quarks. These predictions relied on virtual matrix-elements computed by means of `OpenLoops` [23] and on the subtraction of infrared divergences and NLO QCD + PS matching according to the formalism implemented in `SHERPA` [24]. In particular, `SHERPA` provides its own implementation [25] of the MC@NLO matching scheme [26], together with its own automation [27] of the Catani-Seymour subtraction technique.

In 2016, a dedicated comparison between predictions produced by the different available tools with NLO QCD + PS accuracy was performed in the context of the Higgs Cross-Section Working Group (HXSWG) [3]. Top quarks were assumed stable in the analysis which was used as a common basis for this comparison. For many of the considered distributions, predictions by

OpenLoops + SHERPA in the 4 FNS were found to be in reasonable agreement (i.e. in agreement within factorization and renormalization scale uncertainties) with those by PowHel + PYTHIA [28] in the 5 FNS. However, the question on the agreement between $t\bar{t}b\bar{b}$ predictions in the 4 FNS and 5 FNS remained somehow open, and the issue arose whether possible accidental effects could have played a relevant role, even taking into account that different NLO QCD + PS matching schemes and SMC generators (POWHEG vs. MC@NLO matching and PYTHIA vs. SHERPA) were used in the comparison. Additionally, it was remarked that contributions of diagrams involving double collinear gluon to $b\bar{b}$ splittings, one of which is included at the hard-scattering level, were missing in the 5 FNS computation, and these contributions, present in the 4 FNS computation, were claimed to be important [3, 22]. As a step to contribute to the debate on these open issues¹, we present in this letter a $t\bar{t}b\bar{b}$ PowHel generator based on the 4 FNS, new and complementary with respect to our previous implementation limited to the 5 FNS, and we show predictions obtained in the 4 FNS by use of this tool. These developments open the road to a systematic, consistent and extended comparison between 4 FNS and 5 FNS predictions in the context of the same generator. Here we limit ourselves to show an illustrative comparison between the new predictions in the 4 FNS with previously published ones in the 5 FNS, obtained on the basis of the new and old PowHel versions, respectively, both interfaced to PYTHIA. To test the performances, the reliability and provide a benchmark for the new 4 FNS PowHel event generator, instead of the HXSWG analysis, we consider a more realistic case study, i.e. we perform an analysis of $t\bar{t}b\bar{b}$ hadroproduction with $t\bar{t}$ -quark pairs decaying into the dileptonic channels, using the cuts proposed by the CMS collaboration in Ref. [21]. Besides t -quark decays, we include parton shower, hadronization and multiple particle interaction (MPI) effects, as implemented in the same PYTHIA [29] release already used in Ref. [21], to facilitate the comparison. We stress that even adopting more recent PYTHIA implementations does not modify the conclusions of this work. The scale uncertainties are computed explicitly, as well as the b -quark pole-mass uncertainties so far systematically neglected in previous $t\bar{t}b\bar{b}$ computations in the 4 FNS.

¹ We are aware about a work in progress by an independent group, who is also producing predictions with NLO QCD + PS accuracy for $t\bar{t}b\bar{b}$ hadroproduction with massive b -quarks, using the POWHEG matching formalism. For a recent overview of their results, see e.g. T. Jezo's talk at the QCD@LHC 2017 Workshop, <http://qcdatlhc2017.phys.unideb.hu>.

II. DETAILS OF THE IMPLEMENTATION IN THE 4 FNS

As already mentioned in the Introduction, the Helac-1loop numerical program has been used in the PowHel interface to compute the matrix-elements required as an input of POWHEG-BOX. The $t\bar{t}b\bar{b}$ implementation described in this work follows a recent extension of the public version of the Helac-1loop code [7], to deal with the treatment of the 4 FNS for arbitrary processes. The resulting matrix-elements were checked and agree with those provided by independent generators, i.e. GoSam [30] and RECOLA [31].

Fixed-order $t\bar{t}b\bar{b}$ NLO QCD predictions computed by PowHel in the 4 FNS were compared to those from an advanced version of Helac-NLO (Helac-1loop + the latest public release of Helac-Dipoles [32]), which makes use of two independent formalisms for the subtraction of infrared divergences: the Catani-Seymour and the Nagy-Soper scheme [32–34]. The predictions obtained by the three implementations showed perfect agreement among each other. Different sets of cuts and differential distributions were considered in these comparisons. We checked that our fixed-order (LO and NLO) cross-sections are also in agreement with those reported in Ref. [22].

Further new advanced features of PowHel were exploited for obtaining the results presented in this letter, like the automation in the generation of the Born phase-space, which is also an input for POWHEG-BOX, for generic multileg processes.

In the following we describe the various inputs for the generation of $t\bar{t}b\bar{b}$ PowHel events with massive bottom quarks, used for the phenomenological analysis described in Section III.

Hard-scattering matrix-elements in the 4 FNS are consistently combined with 4-flavour PDFs. In particular, we consider the 4-flavour versions of both the CT10n1o [35] and NNPDF3.0_n1o [36] PDFs. This specific choice is solely triggered by the fact that these PDFs (in their Variable FNS version, involving up to 5 active flavours) were used by our group in our previous $t\bar{t}b\bar{b}$ computations with massless b -quarks at LHC energies. Of course, extending the present computation to other 4 FNS PDF sets is straightforward and can be useful for a more comprehensive estimate of PDF related uncertainties.

Central factorization and renormalization scales are fixed to the values suggested in the $t\bar{t}b\bar{b}$ study of the last HXSWG report [3], i.e. $\mu_{F,0} = 1/2 H_{\perp} = 1/2 \sum_{i=t,\bar{t},b,\bar{b},j} E_{\perp,i}$ and $\mu_{R,0} = (\prod_{i=t,\bar{t},b,\bar{b}} E_{\perp,i})^{1/4}$, respectively, with $E_{\perp,i}$ defined as the transverse energy of each parton-level final-state particle using the real-emission kinematics for the real emission (j labels the first additional radiative emission) and subtractions, and the underlying Born kinematics for all the other contributions. Scale uncertainties are evaluated by varying independently $\mu_R = \xi_R \mu_{R,0}$ and $\mu_F = \xi_F \mu_{F,0}$ in the interval $\xi_R, \xi_F \in [1/2, 2]$, considering the seven-point prescrip-

tion [37] which excludes the extreme combinations (0.5, 2) and (2, 0.5).

The b -quark pole-mass parameter is fixed to $m_{b,0}^{\text{pole}} = 4.75$ GeV, very close to the value which arises from the conversion at 2-loops of the b -quark mass value in the modified minimal subtraction ($\overline{\text{MS}}$) scheme reported in the Particle Data Group review [38] to the on-shell mass scheme ($m_b^{\overline{\text{MS}}}(m_b) = 4.18$ GeV, corresponding to $m_b^{\text{pole}} = 4.78$ GeV). Taking into account that the conversion of $m_b^{\overline{\text{MS}}}(m_b)$ at 1, 2, 3, ... loops gives rise to different m_b^{pole} values, showing only a slow convergence (at least up to 4 loops) [39], we assume as maximum uncertainty on the bottom mass in the on-shell scheme a value slightly larger than the difference between the m_b^{pole} values coming from the conversion to the on-shell scheme of $m_b^{\overline{\text{MS}}}(m_b)$ at 1- and at 2-loops, i.e. approximately 0.25 GeV. We believe that varying m_b^{pole} in an interval $[-0.25, +0.25]$ GeV with respect to the central value provides an estimate conservative enough for the m_b^{pole} uncertainty.

On the other hand, the t -quark pole-mass parameter is fixed to $m_t^{\text{pole}} = 172.5$ GeV², and its uncertainty neglected, as in Ref. [3].

One of the parameters characterizing the POWHEG-BOX (and PowHel) matching uncertainties is h_{damp} , which allows to split the NLO real contribution into a singular part and a part damped in the singular region and thus treatable as a finite remainder which does not enter in the exponent of the Sudakov form factor [41]. To obtain our predictions the following h_{damp} definition has been used: $h_{\text{damp}} = \frac{E_{\perp,t} E_{\perp,\bar{t}}}{p_{\perp,j}^2 + E_{\perp,t} E_{\perp,\bar{t}}} \Theta \left((E_{\perp,t} E_{\perp,\bar{t}} E_{\perp,b} E_{\perp,\bar{b}})^{1/4} - p_{\perp,j} \right)$ where $E_{\perp,i}$ are defined as above and $p_{\perp,j}$ denotes the transverse momentum of the extra parton (first radiative emission). This choice implies that the transverse-momentum distribution of the extra parton approaches the fixed-order one in the tail after the Sudakov shoulder. Studying the effect of h_{damp} variation and of other contributions to the NLO + PS matching uncertainties is certainly interesting and requires a dedicated work beyond the scope of the present letter.

III. PHENOMENOLOGICAL ANALYSIS OF $t\bar{t}b\bar{b}$ HADROPRODUCTION AT THE LHC

We apply the sets of cuts described in the CMS analysis of $t\bar{t}$ hadroproduction in association with at least 2 b -jets at $\sqrt{s} = 8$ TeV [21], requiring that $t\bar{t}$ -quark pairs decay into the e^+e^- , $\mu^+\mu^-$ and $e^\pm\mu^\mp$ dileptonic channels, to

samples of events generated by PowHel + PYTHIA. The decay products of τ^\pm leptons are also allowed to contribute to the aforementioned dileptonic final states.

In this analysis b -jets are distinguished in different categories according to their origin, considering that different sources of b -quarks are possible: b -quarks can be either produced in the partonic hard-scattering process, or by $g \rightarrow b\bar{b}$ splittings in the PS evolution, or by $t \rightarrow W^+b$ decays. Additionally, they can be produced by MPI. In the massless limit, b -quarks from initial state PDFs may also participate in the hard-scattering process or contribute to jets including beam-remnant partons. In the simulation, the origin of the various B -hadrons appearing at hadron level, identifying b -jets, is tracked back by taking into account the Monte Carlo information (mother/daughter chains) in the PYTHIA event records, according to the HEPEVT standard [42]. The decays of t -quarks are also handled by PYTHIA.

Two different sets of cuts after SMC are defined, according to the procedure developed for the CMS analysis [21]. A stricter one, corresponding to the visible phase-space, characterized by two leptons with $p_{\perp,\ell} > 20$ GeV and $|\eta_\ell| < 2.4$ arising from the decay of the $t\bar{t}$ pair, and at least four b -jets, out of which two comes from top decays, and the other two include B -hadrons from b -quarks radiated before top decays. The b -jets from top decays are required to have $p_\perp > 30$ GeV and $|\eta| < 2.4$, whereas the additional b -jets must satisfy the $p_\perp > 20$ GeV and $|\eta| < 2.4$ conditions. On the other hand, a looser system of cuts, corresponding to the so-called full phase-space, requires just to have a $t\bar{t}$ pair decaying into one of the aforementioned dileptonic channels (without explicit cuts on $p_{\perp,\ell}$ and $|\eta_\ell|$), and only imposes cuts on the number (≥ 2), p_\perp and $|\eta|$ of the additional b -jets. The experimental results in the full phase-space, as well as the theory predictions, are corrected a-posteriori for dileptonic branching fractions including τ leptonic decays. In all cases, the anti- k_T clustering algorithm [43] with $R = 0.5$ is used to identify the jets. Further details on the analysis and subtleties in the definition and classification of b -jets can be found in the CMS study [21].

Total cross-sections after MPI in the different dileptonic channels, together with their uncertainties due to μ_R and μ_F scale variation and m_b^{pole} variation, evaluated according to the methods discussed in Section II, are shown in Fig. 1. Scale uncertainties amount to approximately (-30%, +38%) in all dileptonic channels for both systems of cuts (visible phase-space and full phase-space), whereas m_b^{pole} uncertainties, estimated by consistently varying m_b^{pole} around its central value $m_{b,0}^{\text{pole}}$ both in the matrix-elements and in the SMC, are limited within (-3%, +4.5%).

Including MPI effects turns out to enhance the cross-sections after cuts by approximately 8% in the visible phase-space, and 10.5% in the full phase-space. These results are moderately sensitive to the tune adopted. In the PowHel simulations for this letter, like in those made to produce the predictions published in the CMS paper [21],

² We verified that modifying its central value to $m_t^{\text{pole}} = 173.2$ GeV, according to the Tevatron CDF and D0 combination of Ref. [40], has a very mild impact on LO cross-sections.

the PYTHIA p_T -ordered tune Perugia 2011 C [44] was employed.

Besides computing total cross-sections, we produce several differential distributions, considering both the characteristic bin sizes actually used in the experimental analysis, which allows to appreciate the actual experimental capabilities and offers the opportunity of a first comparison with the experimental data, and thinner bins, which better allow to disentangle the shape of distributions and differences between theoretical computations based on different assumptions. For illustrative purposes, we also show a comparison of our new predictions in the 4 FNS with the ones obtained by PowHel in the 5 FNS from an earlier publication [21]. This can be considered just as a first attempt of comparison, because of some differences in some of the inputs used in the two computations, as we will better explain in the following.

When considering the typical experimental bin sizes, as shown in Fig. 2 and 3, differential cross-sections in the 5 FNS turn out to lie within the scale uncertainty bands of those in the 4 FNS (and viceversa). This general conclusion is not biased by the fact that, for the generation of the 5 FNS PowHel events used in Ref. [21], a different set of central scales, in its complex slightly softer than the 4 FNS choice discussed in Section II, was adopted, i.e. $(\mu_{R,0}, \mu_{F,0}) = (H_\perp/4, H_\perp/4)$, with H_\perp computed from the underlying Born kinematics. Furthermore, we observe that a parallel variation of the (μ_R, μ_F) scales around their central values leaves the shape of the considered differential distributions essentially unchanged and that predictions according to the $(\xi_R, \xi_F) = \{(1/2, 1), (1, 1/2), (1, 2), (2, 1)\}$ choices, in general, turn out to be included in the uncertainty bands built considering the parallel choices $(\xi_R, \xi_F) = (1/2, 1/2)$ and $(2,2)$. Scale uncertainty bands are characterized by an approximately constant size around the considered central predictions. This size does not vary in a considerable way from distribution to distribution. A similar behavior is also observed in the case of the 5 FNS. Although we need a more detailed analysis to quantify its exact impact, we believe that the difference in the scales used as input for our 4 FNS and 5 FNS computation plays a minor role in the discussion we present in the following.

The differences in the shapes of the central predictions in the 4 FNS and 5 FNS reported in Fig. 2 and 3 turn out to be smaller than scale uncertainties. However, when considering thinner bin sizes, differences in shape can be better appreciated, as can be seen in Fig. 4, 5 and 6. In particular distributions in the 4 FNS turn out to be harder than those in the 5 FNS, as a consequence of the different m_b and h_{damp} treatment. While in the 4 FNS computation h_{damp} was fixed as explained in Section II, in the 5 FNS computation, done with an older version of the PowHel generator [15], no h_{damp} was set up. The combined effect of these factors is particularly remarkable in case of the m_{b_1, b_2} distribution, where, for $m_{b_1, b_2} \simeq 400$ GeV, predictions in the 4 FNS are $\sim (12 - 25)$ % larger than those in the 5 FNS, depending on the

system of cuts. For larger invariant masses the differences may increase and can exceed the size of the scale uncertainty bands accompanying the 4 FNS predictions. As first noticed in Ref. [22], the contribution of the diagrams with double gluon to $b\bar{b}$ collinear splittings, with one splitting generated at the hard-scattering level, also plays a role in the tails of this distribution. However, when considering the fact that even the 5 FNS predictions are characterized by a scale uncertainty band (not shown in our plots) of size comparable to the 4 FNS band, the predictions in the 4 FNS and 5 FNS can still be considered compatible, at least at the present level of accuracy, according to the fact that the uncertainty bands still overlap.

In Fig. 4, 5 and 6, we also show the comparison between 4 FNS predictions with and without MPI effects. In particular, the inclusion of MPI effects produces shape distortions which are far less pronounced than those described above, seen when comparing our predictions in the 4 FNS and the 5 FNS approximations.

For the differential cross-sections shown in Fig. 2 and 3, the contribution to the uncertainty due to m_b^{pole} variation in the 4 FNS amounts to a few percents. This is certainly of minor importance with respect to scale uncertainties, but it can become of some relevance when one aims at precise comparisons of 4 FNS and 5 FNS predictions.

Finally, the differences related to the use of different PDF sets (the central member of the NNPDF30_nlo_as_0118_nf_4 set vs. the central member of CT10nlo_nf4 in the 4 FNS simulation) turn out also to be limited to very few percent and do not cause relevant shape distortions, as shown in Fig. 2 and 3. Of course, a more detailed analysis of PDF uncertainties, beyond the scope of this letter, requires the generation of events for each of the different PDF members in each given set.

IV. CONCLUSIONS

We have developed a PowHel generator dedicated to $t\bar{t}b\bar{b}$ production with massive b -quarks (4 FNS) at hadron colliders. To demonstrate its capabilities, we have shown a few theoretical predictions at the differential level, obtained after interfacing PowHel to a SMC program (PYTHIA), in the context of a realistic experimental analysis.

A comparison with earlier predictions, based on the same experimental setup and making use of a PowHel generator with massless b -quarks (5 FNS) interfaced to the same SMC, exhibits a reasonable level of agreement within the theoretical uncertainties.

A closer scrutiny at the analysed observables shows examples where the distributions in the 4 FNS are harder in shape than in the 5 FNS. This is not only due to the different treatment of b -quark masses in the two schemes. In the POWHEG-BOX framework, the shape of distributions is affected by the choice of h_{damp} . Therefore, part of these

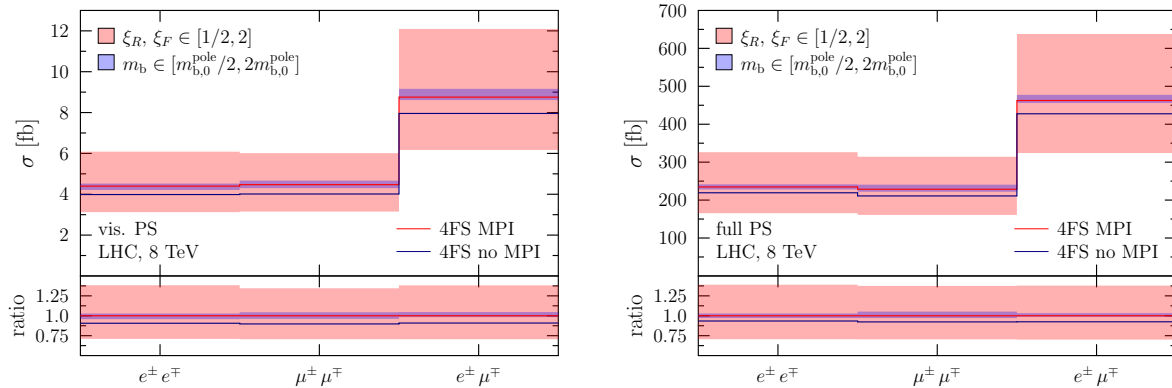


FIG. 1: Total cross-sections for the production of a $t\bar{t}$ -quark pair decaying dileptonically, in association with at least 2 additional b -jets, under the system of cuts defining the visible (*left*) and the full (*right*) phase-space of the CMS analysis of Ref. [21], as predicted at NLO QCD + SMC accuracy by the `PowHel1` + `PYTHIA` implementation of this work, including massive b -quarks for the $pp \rightarrow t\bar{t}b\bar{b}$ process at $\sqrt{s} = 8$ TeV. The central member of the of `NNPDF30_nlo_as_0118_nf_4` PDF set has been used as `PowHel1` input. Predictions including PS, hadronization and MPI effects, accompanied by their uncertainty bands related to scale and m_b^{pole} variation, are compared to those after hadronization, neglecting MPI. In the lower part of each panel all predictions are normalized with respect to the central one, including MPI effects.

differences can be ascribed to the different treatment of the splitting and exponentiation of the real-correction contributions that we have adopted in the 4 FNS computation, in comparison with our earlier one, based on the 5 FNS, which did not make use of the h_{damp} factor.

Our developments open the road to fully consistent and extended comparisons between $t\bar{t}b\bar{b}$ predictions obtained by theoretical computations with matrix-elements with either massive or massless b -quarks, by use of the same generator with NLO QCD + PS accuracy, beyond the illustrative example that we have presented in this letter.

In addition, we have provided for the first time for this process a quantitative estimate of the theoretical uncertainties stemming from the imprecise knowledge of the b -quark mass parameter in the on-shell renormalization scheme. These uncertainties turn out to be much smaller than scale uncertainties.

Similarly, the difference between predictions based on the different PDF sets considered here is subleading with respect to scale variation.

We leave the exploration of further sources of uncertainties, in particular those related to the NLO + PS matching, as well as the analysis of different kinematical setups, to a future publication.

The results of this paper point to a reasonable level of agreement between the predictions based on the 4 FNS and the 5 FNS. Scale uncertainties appear large enough to overcome the differences between the two schemes. We believe that our results support the hypothesis that the agreement found between the predictions of `PowHel1` + `PYTHIA` and `OpenLoops` + `SHERPA` published

in the 2016 HXSWG report is not driven by accidental effects and thus should not be considered as surprising. Clearly, the last word is left to a more detailed analysis of this case-study, now facilitated by the new developments presented in this letter.

The $t\bar{t}b\bar{b}$ `PowHel1` generator with massive b -quarks is made available to the experimental collaborations upon request.

Acknowledgements

We are grateful to the $t\bar{t}H$ conveners of the Higgs Cross Section Working Group, in particular Laura Reina and Stefano Pozzorini, for having equipped us with many motivations and the encouragement to extend our $t\bar{t}b\bar{b}$ `PowHel1` generator to the massive b -quark case. We are indebted to the CMS and ATLAS experimentalists for having manifested continuous interest in our work. We are grateful to Zoltán Trócsányi and Emanuele Bagnaschi for their key contributions to the `PowHel1` project and code, used as a basis for the developments described in this letter. We are grateful to Nicolas Greiner, Sven-Olaf Moch and Michael Benzke for useful discussions. The research of G.B. and A.K. was supported by grant K 125105 of the National Research, Development and Innovation Office in Hungary. A.K. kindly acknowledges financial support through the Premium Postdoctoral Fellowship Programme of the Hungarian Academy of Sciences.

[1] S. Dittmaier *et al.*, (2012), 10.5170/CERN-2012-002, arXiv:1201.3084 [hep-ph] .

[2] J. R. Andersen *et al.* (LHC Higgs Cross Section

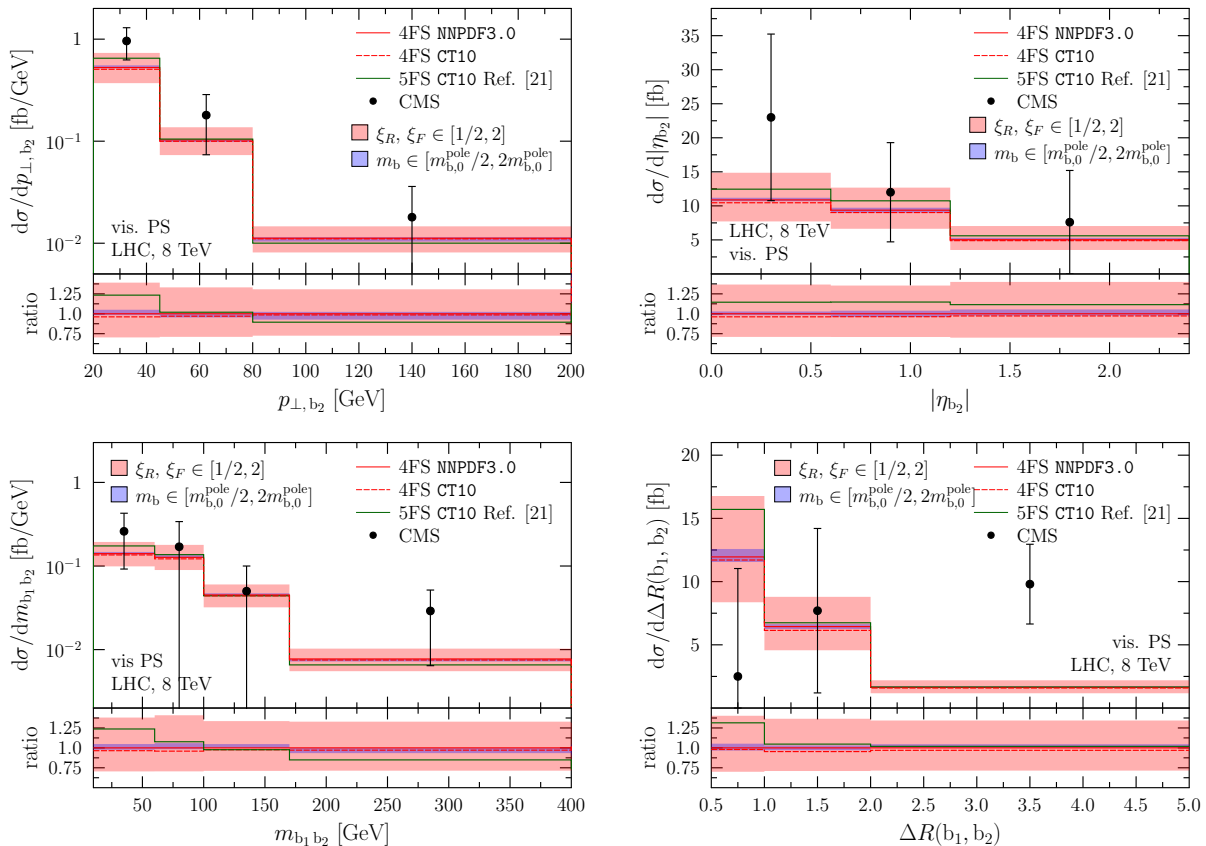


FIG. 2: Differential distributions after MPI for the transverse momentum and the absolute pseudorapidity of the second hardest additional b -jet (upper panels), as well as for the invariant mass and the azimuthal angle - pseudorapidity separation of the two hardest additional b -jets (lower panels), in the visible phase-space of the CMS analysis of Ref. [21]: theory predictions with massive b -quarks obtained in this work (4 FNS) are compared with theory predictions with massless bottom in the hard-scattering matrix-elements (5 FNS), also computed by `PowHel1` + `PYTHIA` and already shown in Ref. [21]. Scale and m_b^{pole} uncertainties affecting theory predictions with massive b -quarks are reported, as well as predictions for the central member of two different PDF sets (the 4 FNS versions of `CT10n1o` and `NNPDF3.0_n1o`). CMS data as published in Ref. [21] are also shown, accompanied by their total uncertainties. In the lower part of each panel all predictions are normalized with respect to the central 4 FNS one, obtained using as input the central member of the `NNPDF30_n1o_as_0118_nf_4` PDF set.

- Working Group), (2013), 10.5170/CERN-2013-004, arXiv:1307.1347 [hep-ph].
- [3] D. de Florian *et al.* (LHC Higgs Cross Section Working Group), (2016), 10.23731/CYRM-2017-002, arXiv:1610.07922 [hep-ph].
- [4] A. Bredenstein, A. Denner, S. Dittmaier, and S. Pozzorini, *Phys. Rev. Lett.* **103**, 012002 (2009), arXiv:0905.0110 [hep-ph].
- [5] G. Bevilacqua, M. Czakon, C. G. Papadopoulos, R. Pittau, and M. Worek, *JHEP* **09**, 109 (2009), arXiv:0907.4723 [hep-ph].
- [6] A. Bredenstein, A. Denner, S. Dittmaier, and S. Pozzorini, *JHEP* **03**, 021 (2010), arXiv:1001.4006 [hep-ph].
- [7] G. Bevilacqua, M. Czakon, M. V. Garzelli, A. van Hameren, A. Kardos, C. G. Papadopoulos, R. Pittau, and M. Worek, *Comput. Phys. Commun.* **184**, 986 (2013), arXiv:1110.1499 [hep-ph].
- [8] G. Bevilacqua, M. Czakon, M. V. Garzelli, A. van Hameren, Y. Malamov, C. G. Papadopoulos, R. Pittau, and M. Worek, *Proceedings, 10th DESY Workshop on Elementary Particle Theory: Loops and Legs in Quantum Field Theory: Woerlitz, Germany, April 25-30, 2010*, *Nucl. Phys. Proc. Suppl.* **205-206**, 211 (2010), arXiv:1007.4918 [hep-ph].
- [9] A. van Hameren, C. G. Papadopoulos, and R. Pittau, *JHEP* **09**, 106 (2009), arXiv:0903.4665 [hep-ph].
- [10] M. Czakon, C. G. Papadopoulos, and M. Worek, *JHEP* **08**, 085 (2009), arXiv:0905.0883 [hep-ph].
- [11] A. Kardos and Z. Trócsányi, *J. Phys.* **G41**, 075005 (2014), arXiv:1303.6291 [hep-ph].
- [12] P. Nason, *JHEP* **11**, 040 (2004), arXiv:hep-ph/0409146 [hep-ph].
- [13] S. Frixione, P. Nason, and G. Ridolfi, *JHEP* **09**, 126 (2007), arXiv:0707.3088 [hep-ph].
- [14] S. Alioli, P. Nason, C. Oleari, and E. Re, *JHEP* **1006**, 043 (2010), arXiv:1002.2581 [hep-ph].
- [15] M. V. Garzelli, A. Kardos, and Z. Trócsányi, *JHEP* **03**, 083 (2015), arXiv:1408.0266 [hep-ph].
- [16] S. Frixione, Z. Kunszt, and A. Signer, *Nucl. Phys.* **B467**,

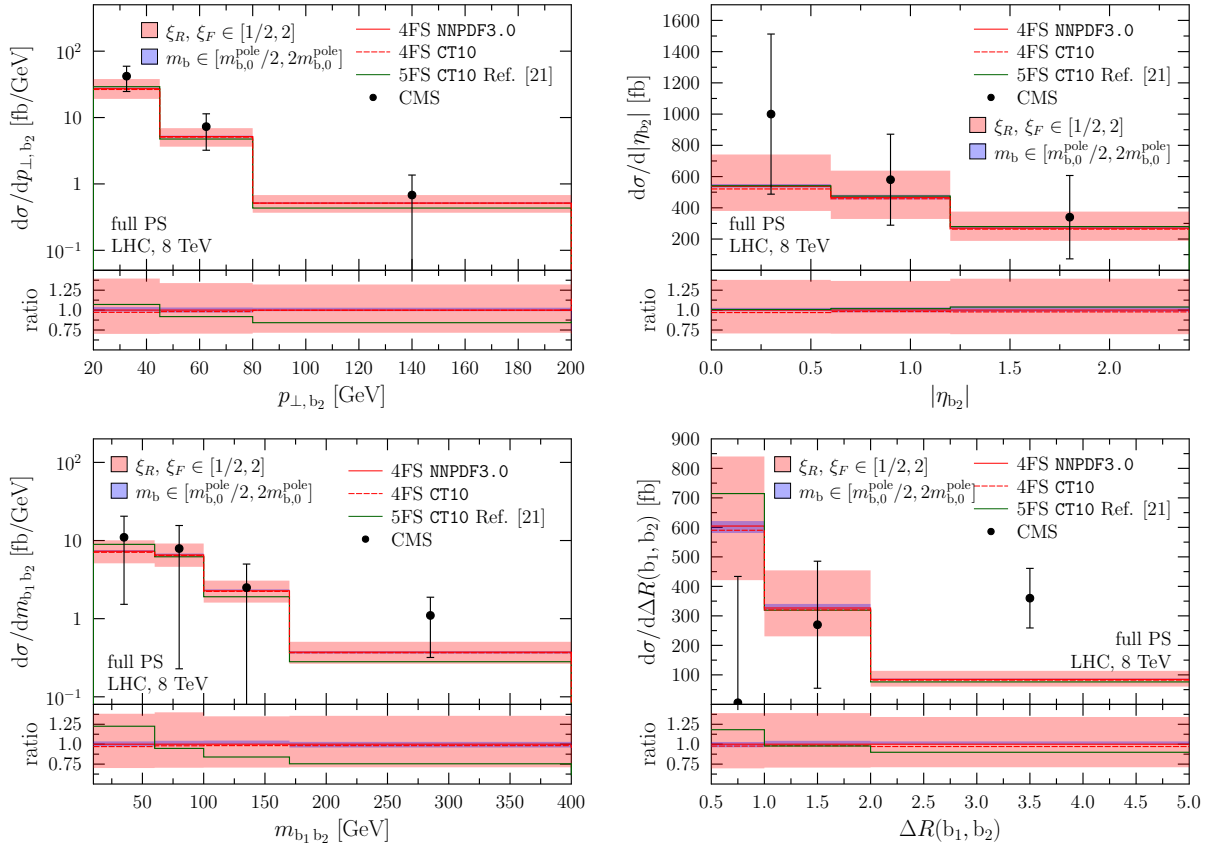


FIG. 3: Same as in Fig. 2, as for the system of cuts corresponding to the full phase-space of the CMS analysis of Ref. [21].

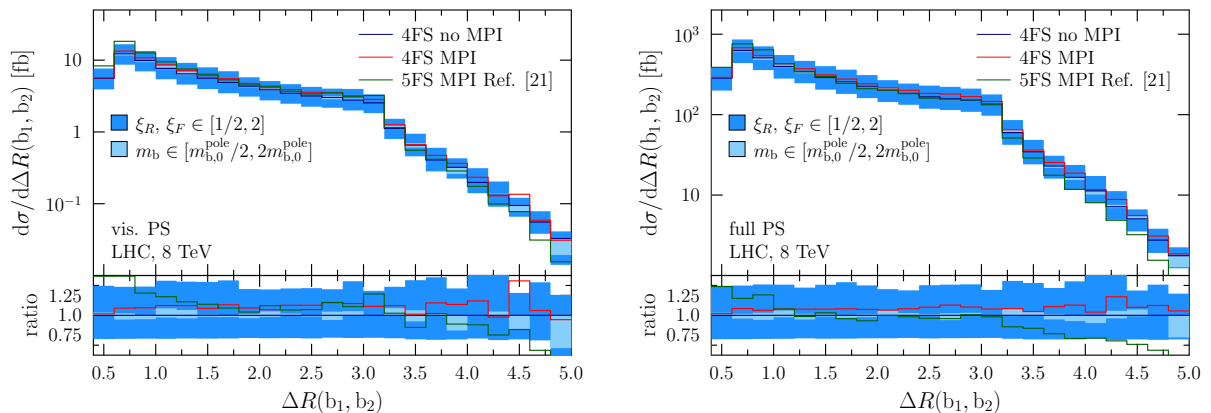


FIG. 4: $\Delta R(b_1, b_2)$ separation between the two hardest additional b -jets for the production of $t\bar{t}$ pairs in association with at least 2 additional b -jets, under the system of cuts defining the visible (*left*) and the full (*right*) phase-space of the CMS analysis of Ref. [21], as predicted by the **PowHel** + **PYTHIA** implementation of this work, including massive b -quarks, for $pp \rightarrow t\bar{t}b\bar{b}$ at $\sqrt{s} = 8$ TeV. Predictions after hadronization but neglecting MPI, accompanied by their uncertainty bands due to scale and m_b^{pole} variation, are compared to those including MPI. Predictions after MPI, obtained from the same **PowHel** events and configuration used in Ref. [21], involving massless b -quarks in the hard-scattering matrix-elements, are also shown. In the lower part of each panel all predictions are normalized with respect to the central 4 FNS one, neglecting MPI effects.

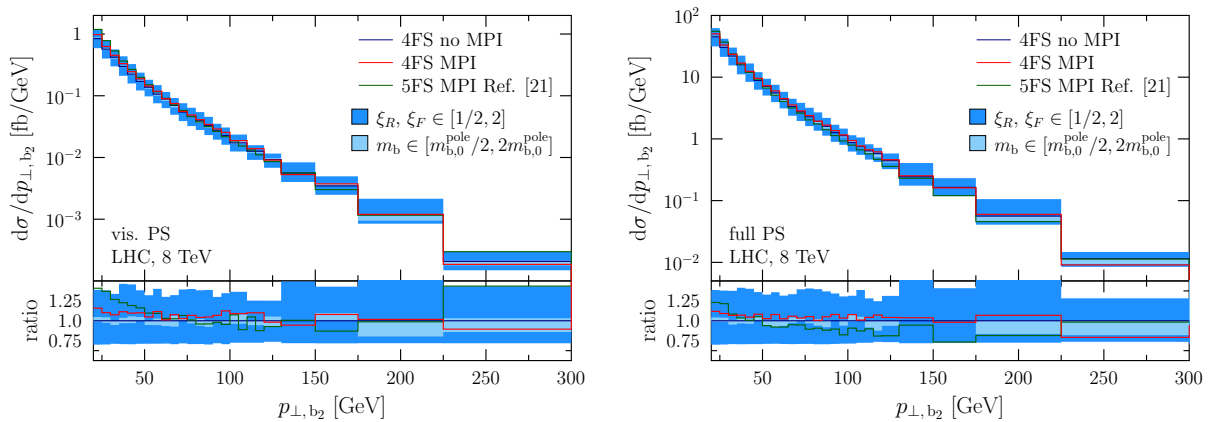


FIG. 5: Same as in Fig. 4, as for the transverse momentum of the second hardest additional b -jet.

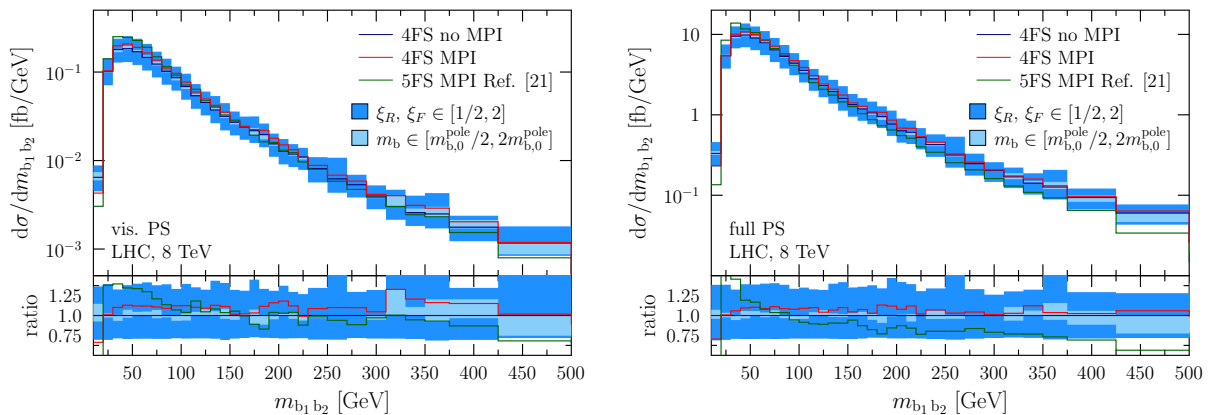


FIG. 6: Same as in Fig. 4, as for the invariant mass of the two hardest additional b -jets.

- 399 (1996), arXiv:hep-ph/9512328 [hep-ph].
- [17] S. Catani and M. H. Seymour, Nucl. Phys. **B485**, 291 (1997), [Erratum: Nucl. Phys.B510,503(1998)], arXiv:hep-ph/9605323 [hep-ph].
- [18] S. Catani, S. Dittmaier, M. H. Seymour, and Z. Trocsanyi, Nucl. Phys. **B627**, 189 (2002), arXiv:hep-ph/0201036 [hep-ph].
- [19] J. Alwall *et al.*, *Monte Carlo for the LHC: A Workshop on the Tools for LHC Event Simulation (MC4LHC) Geneva, Switzerland, July 17-16, 2006*, Comput. Phys. Commun. **176**, 300 (2007), arXiv:hep-ph/0609017 [hep-ph].
- [20] G. Aad *et al.* (ATLAS), Eur. Phys. J. **C76**, 11 (2016), arXiv:1508.06868 [hep-ex].
- [21] V. Khachatryan *et al.* (CMS), Eur. Phys. J. **C76**, 379 (2016), arXiv:1510.03072 [hep-ex].
- [22] F. Cascioli, P. Maierhöfer, N. Moretti, S. Pozzorini, and F. Siegert, Phys. Lett. **B734**, 210 (2014), arXiv:1309.5912 [hep-ph].
- [23] F. Cascioli, P. Maierhofer, and S. Pozzorini, Phys. Rev. Lett. **108**, 111601 (2012), arXiv:1111.5206 [hep-ph].
- [24] T. Gleisberg, S. Hoeche, F. Krauss, M. Schonherr, S. Schumann, F. Siegert, and J. Winter, JHEP **02**, 007 (2009), arXiv:0811.4622 [hep-ph].
- [25] S. Hoeche, F. Krauss, M. Schonherr, and F. Siegert, JHEP **09**, 049 (2012), arXiv:1111.1220 [hep-ph].
- [26] S. Frixione and B. R. Webber, JHEP **06**, 029 (2002), arXiv:hep-ph/0204244 [hep-ph].
- [27] T. Gleisberg and F. Krauss, Eur. Phys. J. **C53**, 501 (2008), arXiv:0709.2881 [hep-ph].
- [28] T. Sjöstrand, S. Ask, J. R. Christiansen, R. Corke, N. Desai, P. Ilten, S. Mrenna, S. Prestel, C. O. Rasmussen, and P. Z. Skands, Comput. Phys. Commun. **191**, 159 (2015), arXiv:1410.3012 [hep-ph].
- [29] T. Sjostrand, S. Mrenna, and P. Z. Skands, JHEP **0605**, 026 (2006), arXiv:hep-ph/0603175 [hep-ph].
- [30] G. Cullen *et al.*, Eur. Phys. J. **C74**, 3001 (2014), arXiv:1404.7096 [hep-ph].
- [31] S. Actis, A. Denner, L. Hofer, J.-N. Lang, A. Scharf, and S. Uccirati, Comput. Phys. Commun. **214**, 140 (2017), arXiv:1605.01090 [hep-ph].
- [32] G. Bevilacqua, M. Czakon, M. Kubocz, and M. Worek, JHEP **10**, 204 (2013), arXiv:1308.5605 [hep-ph].
- [33] Z. Nagy and D. E. Soper, JHEP **09**, 114 (2007), arXiv:0706.0017 [hep-ph].
- [34] C. H. Chung, M. Kramer, and T. Robens, JHEP **06**, 144 (2011), arXiv:1012.4948 [hep-ph].
- [35] H.-L. Lai, M. Guzzi, J. Huston, Z. Li, P. M. Nadolsky, J. Pumplin, and C. P. Yuan, Phys. Rev. **D82**, 074024 (2010), arXiv:1007.2241 [hep-ph].

- [36] R. D. Ball *et al.* (NNPDF), JHEP **1504**, 040 (2015), arXiv:1410.8849 [hep-ph] .
- [37] M. Cacciari, S. Frixione, N. Houdeau, M. L. Mangano, P. Nason, and G. Ridolfi, JHEP **10**, 137 (2012), arXiv:1205.6344 [hep-ph] .
- [38] C. Patrignani *et al.* (Particle Data Group), Chin. Phys. **C40**, 100001 (2016).
- [39] P. Marquard, A. V. Smirnov, V. A. Smirnov, M. Steinhauser, and D. Wellmann, Phys. Rev. **D94**, 074025 (2016), arXiv:1606.06754 [hep-ph] .
- [40] T. A. Aaltonen (Tevatron Electroweak Working Group, CDF, D0), (2013), arXiv:1305.3929 [hep-ex] .
- [41] S. Alioli, P. Nason, C. Oleari, and E. Re, JHEP **04**, 002 (2009), arXiv:0812.0578 [hep-ph] .
- [42] G. Altarelli, R. Kleiss, and C. Verzegnassi, eds., *Z PHYSICS AT LEP-1. PROCEEDINGS, WORKSHOP, GENEVA, SWITZERLAND, SEPTEMBER 4-5, 1989. VOL. 3: EVENT GENERATORS AND SOFTWARE* (1989).
- [43] M. Cacciari, G. P. Salam, and G. Soyez, JHEP **04**, 063 (2008), arXiv:0802.1189 [hep-ph] .
- [44] P. Z. Skands, Phys. Rev. **D82**, 074018 (2010), arXiv:1005.3457 [hep-ph] .